Journal of Catalysis **205,** 86–96 (2002)
doi:10.1006/jcat.2001.3438, available online at http://www.idealibrary.com on IDEAL®

Reactions of *n*-Hexane on Pt Catalysts: Reaction Mechanism as Revealed by Hydrogen Pressure and Compensation Effect

Attila Wootsch[1] and Zoltán Paál

Institute of Isotope and Surface Chemistry, Chemical Research Center of the Hungarian Academy of Sciences, H-1525 Budapest, P.O. Box 77, Hungary

Received May 16, 2001; revised September 17, 2001; accepted October 4, 2001

The reactions of *n*-hexane + hydrogen have been studied using two Pt black catalysts of different preparation (Pt–N, reduced by hydrazine; Pt–HCHO, reduced by formaldehyde). The activities and selectivities were compared with those of EUROPT-1 (6.3% Pt/SiO_2). Maximum rates were observed as a function of hydrogen pressure for the overall reaction as well as for hydrogenolysis, isomerization, C_5-cyclization, and aromatization. Dehydrogenation to hexenes decreased with increasing H_2 pressure. Both Pt black catalysts showed lower turnover frequencies than did EUROPT-1 and the maximum rates appeared at higher hydrogen pressure. The values of Arrhenius parameters calculated in the negative and in the positive hydrogen order range were different for the overall reaction as well as for the individual processes. The apparent activation energies showed compensation effects. Different compensation lines and isokinetic parameters were obtained in the range of positive and negative hydrogen order. The isokinetic parameters indicated that the rate-determining step in the positive hydrogen order may have been a Pt–C bond breaking ("hydrogenative product desorption"), while a C–C bond rupture could be the rate-limiting step in excess hydrogen. The compensation effects of different reactions under different conditions contributes to our knowledge of the reaction mechanism.

Key Words: ***n*-hexane reaction; turnover frequency; hydrogen pressure effect; compensation effect; virtual isokinetic parameters; Pt black; EUROPT-1.**

INTRODUCTION

Hydrogen Effect on the Arrhenius Parameters of n-Hexane Reaction over Pt Catalysts

We reported on the reactions of *n*-hexane over differently prepared, modified, and partly deactivated Pt black catalysts (1–4). The conversion over various Pt catalysts showed maxima as a function of hydrogen pressure in a wide temperature range (1, 5, 6) (i.e., the hydrogen order of the reaction changed from positive to negative with increasing hydrogen pressure). Several explanations have been proposed for this phenomenon. Frennet and coworkers (7–9) postulated the "landing-site model," assuming a multiatomic active ensemble. This hypothesis resulted in maximum rates as a function of hydrogen pressure (9). Bond and Slaa (10–12) used the Langmuir–Hinshelwood bimolecular kinetic theory as an explanation of maximum rates of *n*-butane hydrogenolysis over a Ru/Al_2O_3 catalyst. Accordingly, at lower H_2 pressures the—dissociatively chemisorbed—reactive intermediates compete for hydrogen and the reaction exhibits a positive hydrogen order. Having reached a certain H_2 pressure, the hydrogen coverage reaches an optimum value for the reaction, corresponding to zero hydrogen order. On a further increase of $p(H_2)$, the reacting molecules have to compete with hydrogen for the empty surface sites. Hence, the reaction shows a negative hydrogen order (10).

Skeletal reactions of *n*-hexane over Pt catalysts include four product classes: hydrogenolysis, isomerization, C_5-cyclization, and aromatization. These reactions are accompanied by dehydrogenation to hexenes. The reaction system (1, 5) is more complicated than the hydrogenolysis processes of smaller hydrocarbons (10); hence no *single* model could be proposed to describe *n*-hexane reactions over EUROPT-1 (6.3% Pt/SiO_2) (13). Turnover frequencies (TOF) and Arrhenius parameters could be calculated for the overall reaction as well as for most of the individual processes (i.e., hydrogenolysis, isomerization, C_5-cyclization, and aromatization). The Arrhenius plots calculated for the overall rate at constant hydrogen pressures "bent down" at higher temperatures (13, 14), while those calculated from the maximum rates (corresponding to different hydrogen pressures) gave straight Arrhenius lines (6, 13). We suggested that the latter parameters might approximate the "true" values, although their "apparent" character could not be disproved (13). Large differences were seen between the Arrhenius parameters in the range of positive and negative hydrogen order (13).

The Temkin equations (15) proposed that the apparent activation energy is the sum of the real activation energy and the adsorption enthalpy of the compound multiplied by the reaction order:

$$E_{app} = E_t + \Sigma n_i \Delta H_i. \quad [1]$$

[1] To whom correspondence should be addressed. E-mail: wootsch@alpha0.iki.kfki.hu.

0021-9517/02 $35.00

Equation [1] shows that it is difficult to estimate true activation energies from the measured values. We suggested (13) using the maximum points ($n_i = 0$), while Larsson (16) used zero limiting pressure or concentration ($\Delta H_i = 0$) for calculating kinetic parameters closer to true ones.

Compensation Effect

The linear correlation between activation energy and the preexponential factor in heterogeneous catalysis is called the compensation effect. Compensation phenomena can be observed either when the same reaction is studied on a series of different catalysts or when the same catalyst is used for different reactions (17). Though compensation effect is a widely applied and accepted phenomenon, there is no general interpretation of this behavior (18). Galwey (19) suggested that the main reason may be the energetically heterogeneous surface of the catalyst. There is an exponential dependence between the partial constants and the activation energy on heterogeneous surfaces. The fraction of the corresponding active site depends on the activation energy and gives rise to a compensation effect (19). Another kind of explanation is that the heat and entropy of adsorption are often related to each other in a linear manner (19), because a greater binding energy of the molecule to the surface considerably restricts its vibrational and rotational freedom, as derived mathematically by Balandin (20). Corma *et al.* (21) pointed out that the assumption of the transition state model of the compensation effect means a linear relationship between enthalpy and entropy of the transition state.

The use of Langmuir–Hinshelwood kinetics can also lead to a compensation effect (17, 19). Since the surface coverage of the catalyst by hydrogen and/or reactive hydrocarbon intermediates changes significantly as the temperature increases, the activation energy measured using constant hydrogen pressures can be regarded as "apparent" (E_{app}), while those based on constant surface coverage are labeled "true" (E_t) (17, 22, 23, 24). Compensation effects may occur because of the use of apparent rather than true kinetic parameters (13, 17, 22–24).

Arrhenius plots that obey compensation effects must intersect each other at exactly the same point, defining an "isokinetic temperature" (T_{iso}) and "isokinetic rate" (k_{iso}) (19, 25). Rooney derived the isokinetic parameter from the expanded Eyring equation (26). In his interpretation (26), T_{iso} is correlated with k_{exp}, a ratelike characteristic frequency of the Arrhenius lines resulting in a compensation effect, since, under standard conditions, $k_{exp} = kT_{iso}/h$ (where k is Boltzmann's constant and h is Planck's constant). Larsson (27, 28) and Karpinski and Larsson (29), in turn, correlated T_{iso} with the vibration frequency between the reactant molecule and the catalyst system in complete resonance,

$$T_{iso} \approx 0.715\nu, \qquad [2]$$

where ν is the vibration mode of the reactant molecule (expressed in cm^{-1}) that distorts most strongly the structure of the molecule toward the structure at the activated state (27–29).

The Arrhenius data for the overall consumption of *n*-hexane over EUROPT-1 in the range of negative hydrogen order showed a compensation effect (13) but the point of intersection was out of the range of the real experimental data. We called it a *virtual isokinetic point* (13).

The compensation effect can be used for characterizing heterogeneous catalyst surfaces (22) and can serve as a basis for suggesting a reaction mechanism (19, 22), in spite of the fact that its exact explanation is not proven and that the phenomenon corresponds to apparent rather than to true kinetic parameters (13, 22–24). The reactions that define the same compensation line share common features of reaction mechanisms, for example the same rate-determining step, similar structure of surface intermediates, or analogous types of active centers (19, 22). We reported (13) the effect of hydrogen pressure on kinetic parameters and their compensation phenomenon for EUROPT-1, without drawing any conclusion about the reaction mechanism.

The aim of the present paper is to obtain more information about the effect of hydrogen pressure on kinetic parameters of different Pt catalysts. We want to show that the apparent kinetic parameters as well as their compensation effects can be used for characterizing different catalysts (22). We expect to collect new information on the reaction mechanism of *n*-hexane transformation on Pt catalysts.

METHODS

Catalyst Preparation

Pt black samples were prepared from H_2PtCl_6 using two "classical" methods: reduction with formaldehyde (30) and with hydrazine (31). We adopt an earlier notation (32) and call them Pt–N and Pt–HCHO, respectively.

For preparation of Pt–N, 150 ml of 10% aqueous hydrazine hydrate was added dropwise to a solution of 10 g of H_2PtCl_6 in 8 ml of water over 25 min. A dark-gray precipitate was formed. The liquid was thereafter boiled for 24 h to remove residual ammonia; the Pt was washed with bidistilled water for several days (2).

For preparation of Pt–HCHO, 5 g of H_2PtCl_6 was dissolved in 4 ml of water and mixed with 10 ml of formaldehyde. Then, 16 ml of 50% aqueous KOH was added dropwise, with cooling to ~290 K. The precipitated Pt was washed with HNO_3 to remove residual K and with bidistilled water (3).

Both samples were pretreated in a H_2 flow at 473 K, resulting in a sintered but stable sample (33). The specific surface (BET, N_2) as well as the dispersion (H_2–O_2 titration,

400 K) was measured after the hydrogen treatment. For Pt–N, BET (N_2) = 2.64 m^2/g, and the dispersion was 0.89% (2.73×10^{16} Pt atom on the surface of 1 mg of catalyst). For Pt–HCHO, BET (N_2) = 3.80 m^2/g, and the dispersion was 1.36% (4.20×10^{16} Pt atom on the surface of 1 mg of catalyst).

Catalytic Tests

Catalytic runs were carried out in a closed-loop reactor (volume ~70 ml) described earlier (34). It was filled with a mixture of *n*-hexane (10 Torr) and hydrogen (60–480 Torr). The temperature ranged between 513 and 633 K. The same charge of catalyst was used (16.5 mg of Pt black reduced by hydrazine—with 4.51×10^{17} surface Pt atoms—and 11.2 mg of Pt black reduced by HCHO—4.69×10^{17} surface Pt atoms). Sampling took place after a 5-min reaction time in all cases. Product analysis was performed gas chromatographically using a 50-m CP-Sil glass capillary column (34). The TOFs (35) were calculated as the number of hexane molecules reacted per one surface Pt atom, using the length of the run as the "contact time" (13). Regeneration between the runs was carried out at the reaction temperature with 30 Torr air for 2 min followed by evacuation and a 3-min hydrogen treatment at 100 Torr. When the reaction temperature was changed, two regenerations took place, both at the previous and at the subsequent reaction temperatures. Several catalytic runs were carried out with *n*-hexane + H_2 mixtures, and the catalyst was also regenerated in between. The catalytic properties were well reproducible (typically within ±5%) after several regenerations (36a).

Surface Analysis

The atomic surface composition of the Pt black catalysts (2, 3, 32, 36) was determined by X-ray photoelectron spectroscopy in three states: "as received," after exposure to the *n*-hexane + H_2 mixture (20 min), and after regeneration with 20 Torr of O_2 (5 min) and 200 Torr of H_2 (20 min). These treatments were carried out in the preparation chamber of the photoelectron spectrometer (36) and were analogous to the reaction of the *n*-hexane + hydrogen mixture and subsequent regeneration in a glass reactor. The results of surface analysis are presented in Table 1. Pt–HCHO contained more carbon and oxygen than did Pt–N. The amount of carbon atoms increased on the surface after exposure to *n*-hexane + H_2. Regeneration removed a fraction of the surface carbon. The surface composition, such as catalytic properties, was well reproducible after several regenerations. The residual surface oxygen after regeneration (on both Pt–HCHO and Pt–N) belonged mainly to adsorbed water and chemisorbed Pt–OH ensembles, with hardly any "Pt–O" and very little oxidized C entities (2, 3, 32).

TABLE 1

XPS Surface Analysis of Pt Black Catalysts (atom %)

Catalyst		Pt	O	C
Pt–N	As received	84	5	11
	Regenerated[a]	78	2	20
	After *n*-hexane exposure[b]	66	1	33
Pt–HCHO[c]	As received	75	11	15
	Regenerated[a]	76	6	18
	After *n*-hexane exposure[b]	68	4	28

[a] Regeneration was carried out, after evacuating the reaction mixture, using 30 Torr of air for 2 min, then evacuating and subsequently using 100 Torr of H_2 for 3 min.

[b] After exposure to $p(nH) : p(H_2) = 10 : 60$ Torr at $T = 603$ K for $t = 20$ min.

[c] Ref. 36b.

RESULTS

Figure 1 shows the overall consumption of *n*-hexane on Pt black catalysts as a function of hydrogen pressure. The shape of these curves resembles earlier analogous results on Pt blacks (2, 3) and on EUROPT-1 (13). The maxima were shifted toward higher hydrogen pressures as the temperature increased. The spline-type curves presented in Fig. 1 are similar to those constructed by a more correct computer simulation for the simpler reaction: butane hydrogenolysis (17).

TOF values were calculated as the number of hexane molecules transformed over one surface Pt (determined by H_2–O_2 titration) per unit time (35). Due to the well-known ensemble effect (37), however, the number of actual active sites is very likely not equal to the number of surface Pt atoms. Figure 2 summarizes the hydrogen pressure dependence of the TOFs on both Pt blacks and EUROPT-1 (13) at three selected temperatures (533, 573, and 603 K). The reaction rate was highest on EUROPT-1 and the lowest on Pt–HCHO. The values of maximum rates represent "the catalytic activity," while the hydrogen pressure of maxima shows the optimum reaction conditions for each temperature (Table 2). They were at somewhat higher values in the case of Pt blacks than of Pt/SiO_2 (EUROPT-1) (Table 2).

The hydrogen dependence of the yield of individual product classes was also examined. The curves of benzene, methylcyclopentane (MCP), and skeletal isomers had maxima over hydrogen pressure. The last two are closely related reactions (38, 39); therefore, as an example, we show the hydrogen pressure dependence of their sum as "C_6 saturated products" in Fig. 3 for Pt–N at all the examined temperatures. Analogous, but lower, values were seen with Pt–HCHO. The optimum conditions were different for each reaction (1) (Table 3). Skeletal isomerization needed the highest optimum hydrogen pressure, while the lowest value appeared for aromatization (Table 3). Hydrogenolysis showed positive and dehydrogenation showed negative

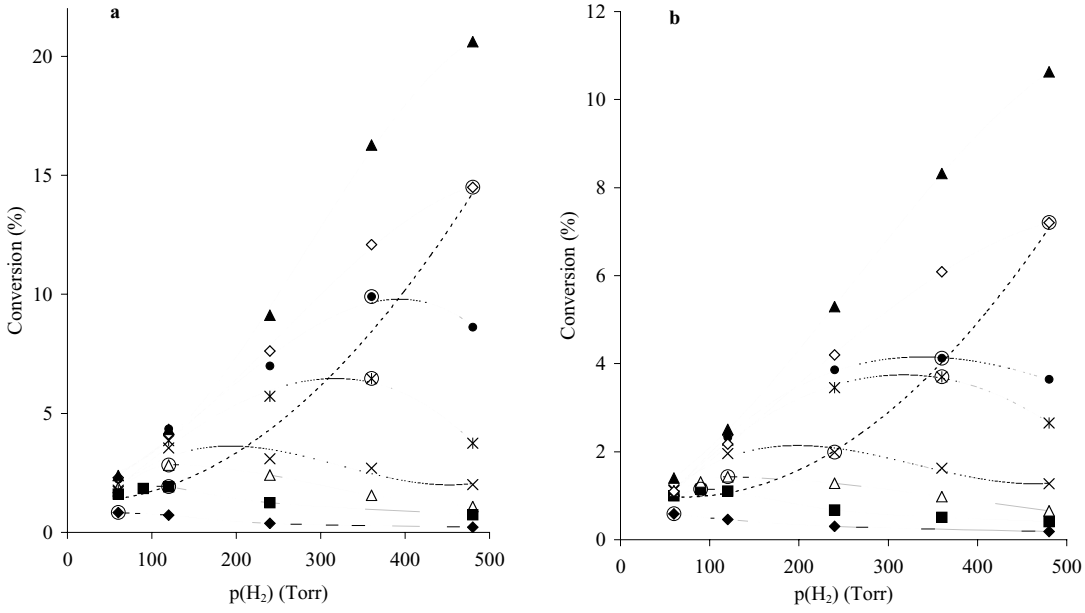

FIG. 1. Conversion (%) of *n*-hexane transformation over Pt black catalysts at different temperatures. (a) Pt–N, (b) Pt–HCHO. The ordinate scale of the two graphs are different. The curves represent the closest fit (spline) curve. Encircled points are the measured ones that are nearest to maxima. The dotted line is a second-order polynom for the maxima of the individual curves. ◆, 513 K; ■, 533 K; △, 543 K; ×, 558 K; ✳, 573 K; ●, 583 K; ◇, 603 K; ▲, 663 K.

hydrogen order under the experimental conditions; thus their optimum hydrogen pressure was not reached.

The selectivities of individual product classes are shown in Fig. 4 at three temperatures (533, 573, and 603 K). EUROPT-1 exhibited higher selectivities for isomers and methylcyclopentane (MCP) and lower values for hydrogenolysis and benzene (34, 40). Dehydrogenation to hexenes was negligible at low temperatures; it became important at low hydrogen pressure and high temperature. Even the highest value (EUROPT-1 at 603 K, $p(H_2) = 60$ Torr) did not exceed 25%. Pt–N resulted in more hexenes, somewhat more fragments of benzene, and less isomers and MCP than did Pt–HCHO.

Arrhenius plots are usually calculated at constant hydrogen pressures. Another possibility is to use maximum rates representing zero hydrogen order. Figure 5 illustrates these results, similar to those reported using EUROPT-1 (13). Different Arrhenius lines could be constructed in the range of negative and positive hydrogen order, respectively. The points taken from the maxima defined an enveloping curve (thick lines in Fig. 5). The calculated

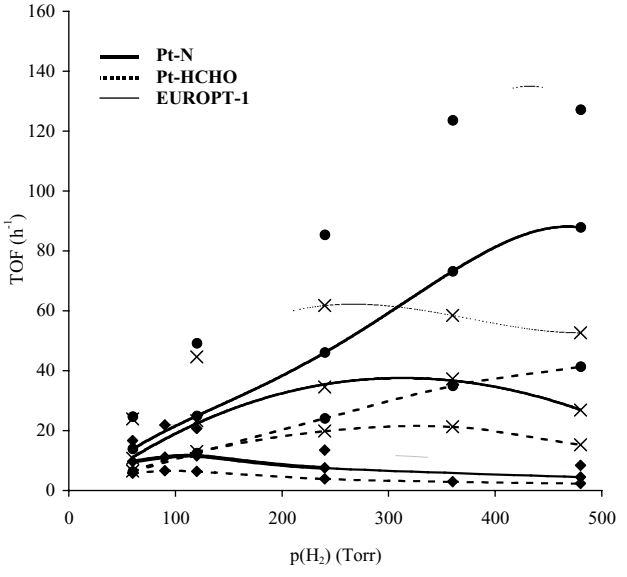

FIG. 2. Comparison of the hydrogen dependence of the overall rate of *n*-hexane transformation over Pt blacks and EUROPT-1 (13) at 533 (●), 573 (×), and 603 K (◆).

TABLE 2

Comparing the Maximum Rates and Their Hydrogen Pressures of Pt Black Catalyst with Standard EUROPT-1

	Pt–N		Pt–HCHO		EUROPT-1[a]	
T (K)	$p(H_2)$ (Torr)	TOF (h^{-1})	$p(H_2)$ (Torr)	TOF (h^{-1})	$p(H_2)$ (Torr)	TOF (h^{-1})
533	118	11.6	115	6.4	97	22.5
543	148	17.1	147	11.5	133	30.1
558	192	22.9	201	21.3	214	45.5
573	315	39.1	320	23.7	257	62.5
583	397	60.0	375	41.5	294	74.7
603	>480	—	>480	—	432	135.0

[a] Ref. 13.

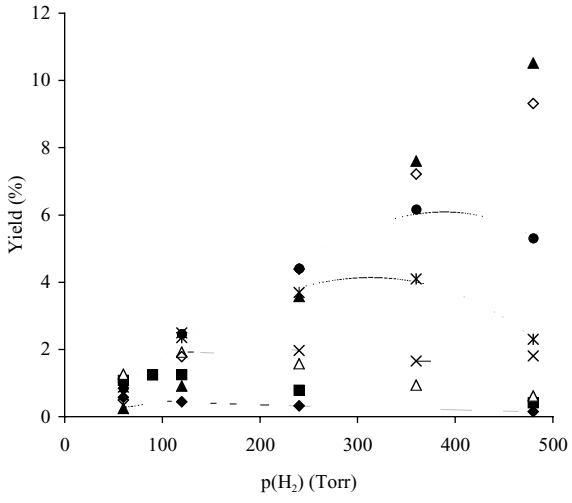

FIG. 3. Yield of saturated C_6 products over hydrogen pressure at various temperatures on Pt–N. ◆, 513 K; ■, 533 K; △, 543 K; ×, 558 K; ✳, 573 K; ●, 583 K; ◇, 603 K; ▲, 663 K.

Arrhenius parameters are presented in Table 4 and compared with the results of EUROPT-1. These parameters are apparent—they are mathematically calculated constants of the Arrhenius lines—and do not have necessarily any physicochemical meaning (13).

It is more difficult to calculate the true activation energies. As predicted from Eq. [1], the apparent energy is independent of ΔH_H when the hydrogen order is zero, but still depends on ΔH_{nH}. The value of the hexane order (n_{nH}) changed from zero to one, depending on temperature and hydrogen pressure (41). From the results reported earlier, $n_{nH} \approx 1$ was between 543 and 633 K for EUROPT-1 at $p(H_2) = 120$ Torr (41). Thus $E_{maximum} \approx E_t + \Delta H_{nH}$. The values can be regarded as close to true values if we apply one single Temkin equation [Eq. 1] for the overall reaction. However, this is a rather rough approximation. Different reactions leading to each product class have their own elementary steps and surface intermediates. Their formal description involves individual Langmuir-type equations, with the three constants (k_1, K_A, K_B) having their own temperature dependence. The E_{app} calculated may eliminate *some* but not *all* distorting factors and thus may be closer to the true value.

We attempted to calculate Arrhenius plots for the individual processes, too. The Arrhenius plots of skeletal isomers, MCP, and ΣC_6-saturated products were "inverted" in the range of positive hydrogen order (Fig. 6) (14). Thus the rate of their formation formally decreased with the temperature so that even apparent Arrhenius parameters could not be calculated. This behavior also appears in Fig. 3, showing at low hydrogen pressure lower yields of C_6-saturated products when the temperature increased. Inverse Arrhenius plots also appeared separately for skeletal isomerization and C_5-cyclization. This phenomenon can be explained by the "hydrogen effect" (1, 22, 42, 43) and carbonaceous deposit formation (44): the hydrogen surface coverage depends on both temperature and hydrogen pressure. The yield and rate of formation of reaction intermediates is a function of the available hydrogen on the surface. Its amount is proportional to the hydrogen pressure at the same time; the "effective surface hydrogen pressure" may be higher than the gas-phase value (45). Besides the gas-phase products residual carbonaceous deposits were also formed during hexane transformation (46). They are the main cause of catalyst deactivation (47). Their appearance is controlled by the available surface hydrogen (44) (i.e., high temperature and low hydrogen pressure, range of positive hydrogen order, favored their formation). Under these severe conditions, high T and low $p(H_2)$, the initial catalytic activity is directed for forming surface carbonaceous deposits rather than products (46). As a consequence (Fig. 5), the Arrhenius curves for the overall reaction bend down (42). C_6-saturated product formation suffers mostly from carbon accumulation, and accordingly their formation reduced significantly on carbonized catalysts (40, 46). Thus inversion of Arrhenius curves appears here (Fig. 6).

TABLE 3

H_2 Pressures of the Maximum Rates for Individual Processes over Pt–N (in Torr)

T (K)	Isomer	MCP	ΣC_6 sat.[a]	Benzene
513	<60	<60	<60	<60
533	100	<60	90	78
543	142	120	135	117
558	150	132	143	130
573	342	285	332	197
583	396	363	381	262
603	>480	>480	>480	362
663	>480	>480	>480	>480

[a] ΣC_6 sat. = skeletal isomers + MCP.

DISCUSSION

Compensation Behavior and Isokinetic Effect

Figure 7 compares the results of Pt black catalysts with the compensation lines reported for EUROPT-1 (13, 48). The points of the overall reaction calculated in the negative hydrogen order range for both Pt black catalysts determine a straight line parallel to those taken from the literature. The differences between the compensation lines can be caused by various things. One of them might be the different dispersion value. The dispersion was measured by H_2–O_2 titration.

Arrhenius parameters calculated in the region of negative hydrogen order for MCP, for skeletal isomers, for benzene, and for ΣC_6-saturated products were compared with earlier results (13, 48). The same was done in the

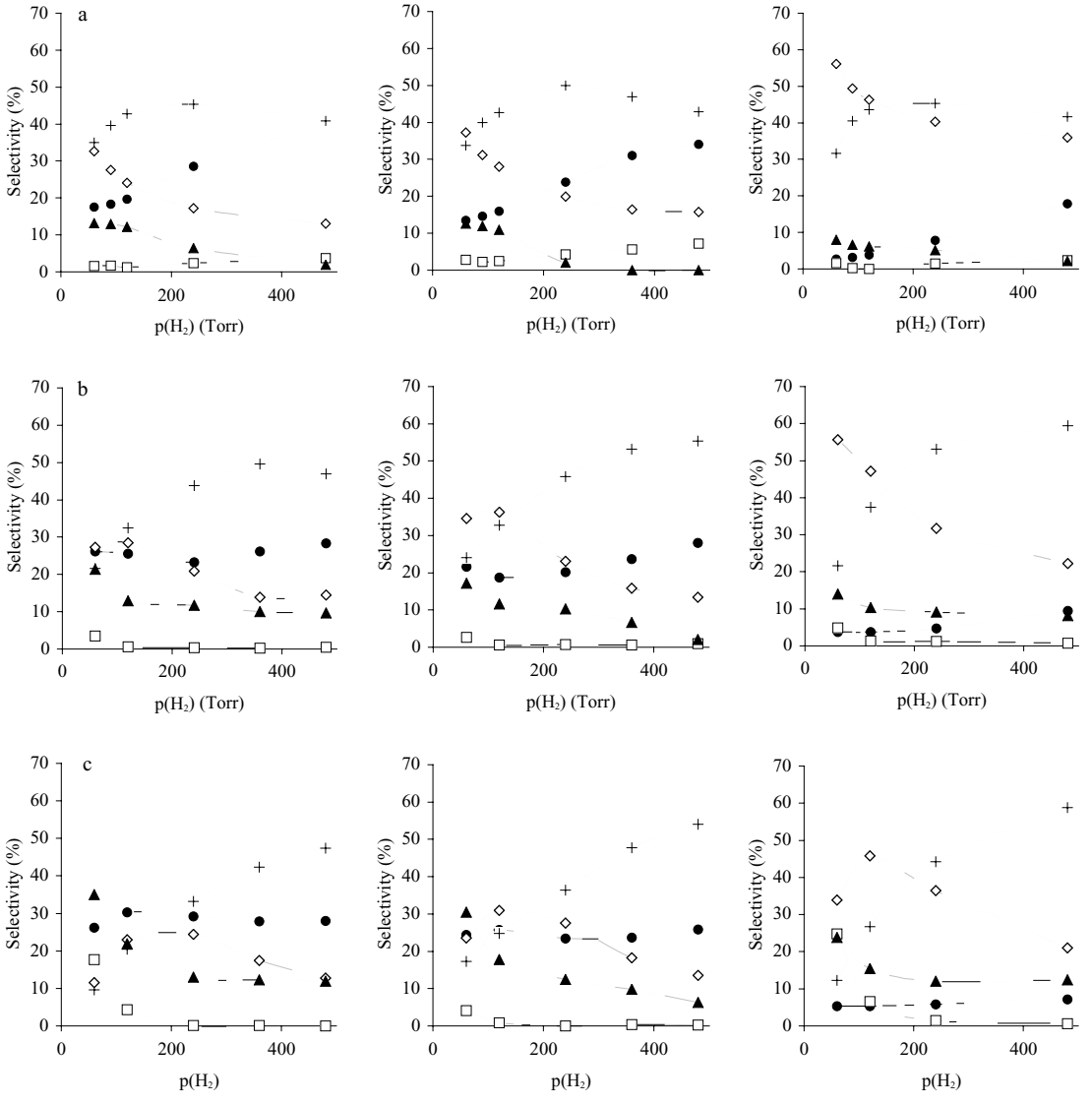

FIG. 4. Selectivity of the individual product classes as a function of the hydrogen pressure (in Torr) over Pt–N (left), Pt–HCHO (middle), and EUROPT-1 (right) at (a) 533, (b) 573, and (c) 603 K. +, Skeletal isomers; ◇, MCP; ▲, benzene; ●, fragments ($<C_6$); □, hexenes.

region of positive hydrogen order for the overall process, hydrogenolysis, and benzene (Fig. 6). The slopes of the compensation lines for the negative and positive hydrogen order ranges were different for all examined catalysts. Further, some points for different reactions lie on the same compensation line, while others do not. In particular, (a) skeletal isomers and ΣC_6-saturated products agree with those of the *n*-hexane overall consumption in the negative hydrogen order range, and (b) the data points for hydrogenolysis lie on a different curve, coinciding with that of aromatization in the positive hydrogen order range.

Reactions that obey the compensation effect can be called *related reactions*, since they have the same kind of a surface intermediate and/or the same rate-determining step (19, 22). The formation of skeletal isomers and C_6-saturated products is on the same compensation line as the overall conversion in the negative hydrogen order for all three catalysts (Fig. 7). Thus, they are *closely related reactions* (34, 38, 39), and their formation (exhibiting highest selectivities) may determine the overall rate of *n*-hexane transformations in the range of the negative hydrogen order (23).

Arrhenius plots that obey the compensation effect ought to intersect each other at exactly the same point, defining an isokinetic temperature and isokinetic rate (19, 25). The Arrhenius lines for EUROPT-1 intersect each other outside the physicochemical range of the actual range of measurements, resulting in so-called *virtual isokinetic parameters* (13). The same phenomenon appears in the case of Pt blacks. The calculated parameters are presented in Table 5.

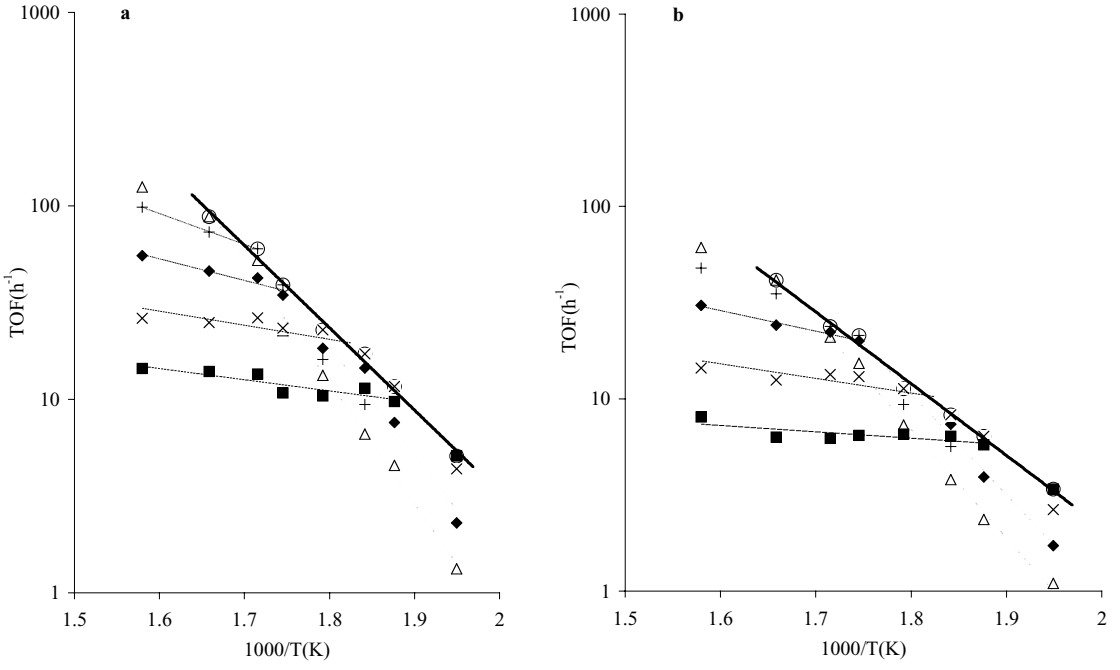

FIG. 5. Arrhenius plots calculated at constant hydrogen pressures over Pt black catalysts: (a) Pt–N, (b) Pt–HCHO. Encircled points correspond to maximum of conversion in Fig. 1. △, 480 Torr; +, 360 Torr; ◆, 240 Torr; ×, 120 Torr; ■, 60 Torr.

The isokinetic parameters calculated from the intersection of compensation lines can also give some information about the likely reactions of adsorbed surface intermediates. Larsson found that the isokinetic temperatures are different over different metals in ethane hydrogenolysis reactions (49, 50), being around 725 K for Ir, Pt, and Ni, and 330–320 K for Co and Fe. The vibration frequencies calculated using Eq. [2] were close to the frequency of a C–C stretch on Ir, Pt, and Ni and to that of a M–C bond stretch on Co and Fe (49, 50). Thus a different reaction mechanism was suggested for the different metals (50): C–C bond breaking was claimed to be rate determining on Pt, Ir, and Ni, and M–C bond breaking was claimed on Fe and Co. This

TABLE 4

Comparison of Overall Kinetic Parameters[a]

Catalyst: H_2 order	$p(H_2)$	Pt–N		Pt–HCHO		EUROPT-1[b]	
		E_{app}	ln(A)	E_{app}	ln(A)	E_{app}	ln(A)
Positive	60	11	4.8	6	3.2	8	4.9
	120	11	5.5	15	5.5	13	6.4
	240	21	8.1	20	7.3	17	7.8
	360	30	10.4	33	10.1	—	—
Zero	Maximum	81	21	71	18	66	18
Negative	60	—	—	—	—	91	23.7
	120	—	—	—	—	102	26.0
	240	107	26.2	94	22.7	115	28.1
	480	120	28.3	107	25.1	117	28.3
Literature[c]	730	—	—	—	—	117	26.8

[a] E_{app} in kJ mol $^{-1}$; A, in h $^{-1}$; $p(H_2)$, in Torr.
[b] Ref. 13.
[c] Ref. 48.

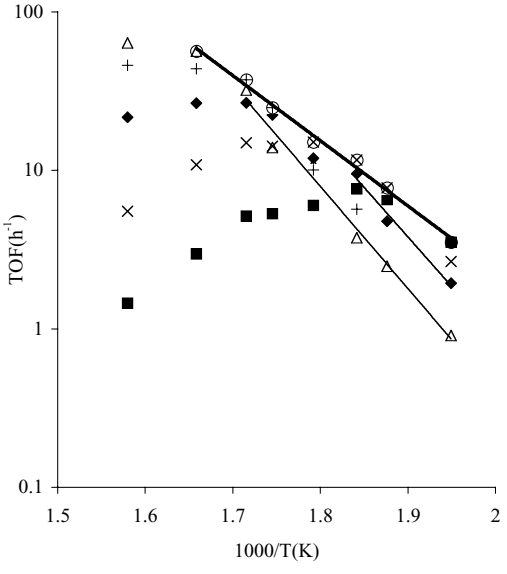

FIG. 6. Arrhenius plots calculated for saturated C_6 at constant hydrogen pressures over Pt–N. Encircled points correspond to maximum of yields in Fig. 5. △, 480 Torr; +, 360 Torr; ◆, 240 Torr; ×, 120 Torr; ■, 60 Torr.

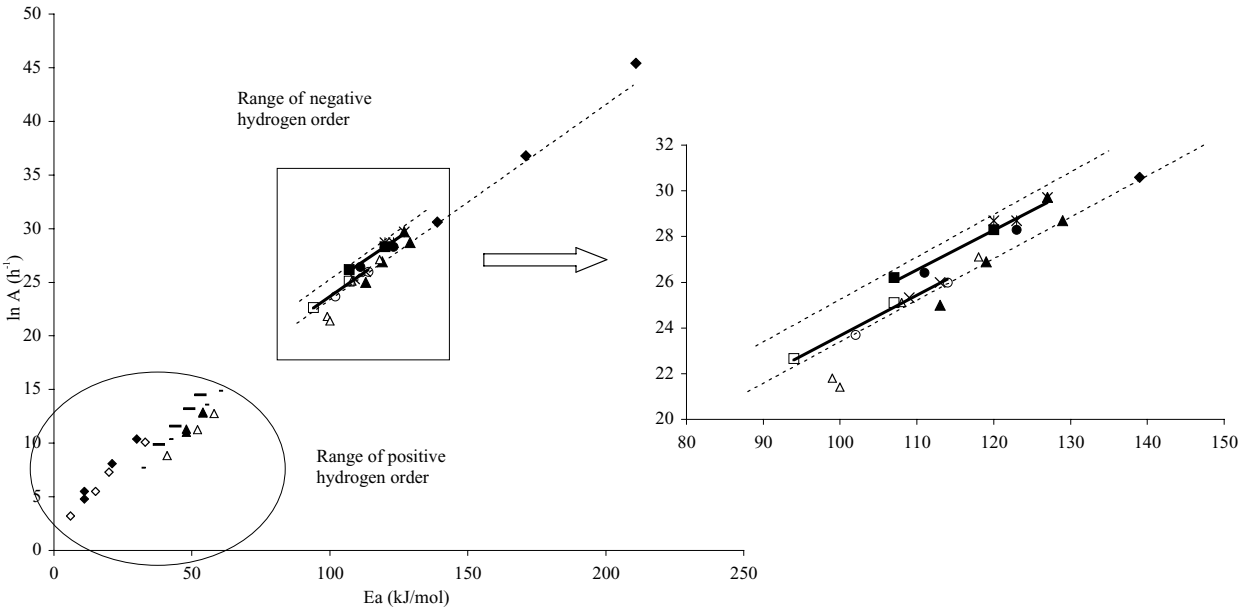

FIG. 7. The compensation effect for *n*-hexane conversion as well as for individual reactions. Earlier results of several reactions (48)—lower dotted line—and our earlier reaction (13)—upper dotted line—on EUROPT-1 are compared with those of the present work. Pt–N: ■, overall reaction; ✳, ΣC_6-saturated products; ●, skeletal isomers; ▲, MCP; ◆, benzene (hydrogenolysis). Pt–HCHO: □, overall reaction; ×, ΣC_6-saturated products; ○, skeletal isomers; △, MCP; ◇, benzene (hydrogenolysis).

latter process represents the decomposition of rather stable surface species.

The present system is more complicated than the ethane hydrogenolysis procedure but the similar isokinetic temperatures may indicate similar frequencies in the transition states. According to Larsson's suggestion, the frequencies calculated from T_{iso} belong to the rate-limiting transformation of the adsorbed surface intermediates (49, 50). The isokinetic parameters presented in Table 5 estimated a frequency close to the value of a C–C bond stretch in the negative hydrogen order and to that of a C–Pt bond stretch in the positive hydrogen order, analogously to Larsson's values on different metals (49, 50). Thus when the hydrogen coverage was low (i.e., in the range of positive hydrogen order), the overall rate-determining step might be the formation or rupture of a C–Pt bond (51). In the range of negative hydrogen order, when hydrogen excess was present on the surface, a C–C bond formation or cleavage appeared to be the rate-limiting step.

TABLE 5

Isokinetic Parameters Calculated from the Compensation Parameters in the Negative and Positive Hydrogen Order Range

	Negative hydrogen order		Positive hydrogen order	
Catalyst	TOF_{iso} (h^{-1})	T_{iso} (K)	TOF_{iso} (h^{-1})	T_{iso} (K)
Pt–N	1760	690	8	440
Pt–HCHO	365	680	6	465
EUROPT-1[a]	850	650	5	320

[a] Ref. 13.

Hydrogen Effect and the Suggested Reaction Mechanism

The suggested reaction mechanism is presented in Scheme 1. The first step can be a—probably rate determining (52)—dissociation of *the first* C–H bond of the saturated reactant (3, 38, 39, 45). Alternatively "reactive adsorption,"

$$C_6H_{14} + PtHPt \rightarrow C_6H_{13}Pt + 2PtH, \qquad [3]$$

can also be assumed (7). This can be the surface

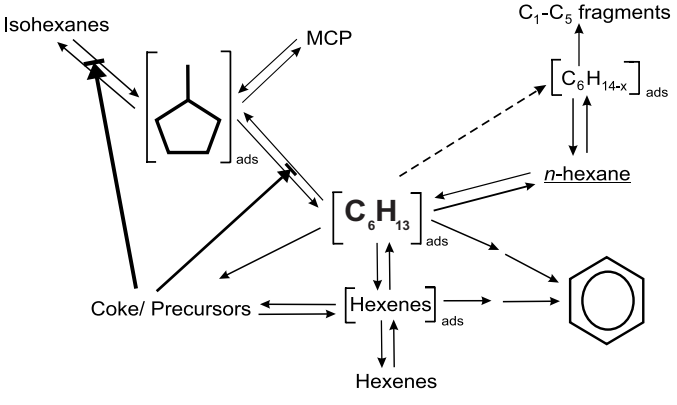

SCHEME 1. The suggested reaction mechanism for the reaction of *n*-hexane over Pt catalysts. The bold lines symbolize the effect of deactivation by carbonaceous deposits (3, 36, 40).

intermediate of the adsorbed C_5-cyclic species, which can react to give MCP or skeletal isomers (Scheme 1) (3, 38, 39). Their ratio is governed by the available surface hydrogen (3, 45, 53, 54). Formation of isomers from the common intermediate needs the uptake of two hydrogen atoms; hence it should be more favored by ample hydrogen availability. Indeed, the isomer/MCP ratio was higher when the back-spillover from the support could increase the amount of hydrogen available on the metal (e.g., on graphite nanofiber-supported Pt catalysts) (55).

Arrhenius parameters of hydrogenolysis lie on a different compensation line. Thus there must be a separate reaction route from the key intermediate (Scheme 1). It was suggested (56) that a "one-point adsorption" of the alkane and its subsequent attack by a neighboring hydrogen can be the route of ethane hydrogenolysis over Pt catalysts. Larsson (50) based his calculations on this assumption. This route is analogous to the formation of the $C_6H_{13}Pt$ key intermediate (Scheme 1 and Eq. [3]) first and its fragmentation without further dehydrogenation. Internal rupture was regarded as closely related to isomerization and may involve a not deeply dehydrogenated intermediate (37b, 57). However, several authors attribute a deeply dissociated (e.g., α, α, γ) intermediate(s) to hydrogenolysis (58), the formation and decomposition of which must involve several elementary steps, more difficult to interpret.

Dehydrogenation to hexenes becomes pronounced (up to 25%, Fig. 4) when a small amount of hydrogen is present on the surface (3) and the number of contiguous metal sites drops (37b). These unsaturated species can desorb as hexenes or form more unsaturated adsorbed molecules like hexadienes or trienes (51, 59). Their *cis* ⇆ *trans* isomerization requires also hydrogen but can still take place with less H(ads) present. Benzene forms via the cyclization of the *cis* trienes (59, 60), while the *trans* isomers can polymerize to carbonaceous deposits (1, 59).

Longer polymeric deposits—precursors of graphitic or C_xH_y entities (32, 36)—are formed more easily on the larger contiguous planes of Pt blacks ($D \approx 1\%$) than on the well-dispersed EUROPT-1 ($D = 60\%$). The different hydrogen content of carbonaceous deposits could also be measured by their deuterative removal (61): the carbonaceous deposits on EUROPT-1 contain more hydrogen than do those on Pt black. This result agrees well with the present selectivity data (Fig. 4): more saturated C_6 products—favored by a "Pt–C–H" state (62)—were formed over EUROPT-1. More benzene and lower catalytic activity were, in turn, found on Pt blacks, in agreement with its easier transformation to a deactivated "Pt–C" state (62).

In the range of positive hydrogen order, benzene formation should need surface hydrogen. The rate-limiting step may be "hydrogenative desorption" of C_6H_6 from C_6H_{6-x} surface entities (51, 60) (i.e., the hydrogenolytic rupture of the surface Pt–C bond). This is in agreement with the results calculated from the isokinetic parameters. On the other hand when much hydrogen is present (negative hydrogen order), dehydrogenation to unsaturated surface intermediates of aromatization can be hindered (1, 45, 59).

The hydrogen pressure at maximum rates defines the optimum hydrogen coverage. This is higher over Pt blacks than over Pt/SiO_2 (Fig. 2). Hydrogen spillover facilitates hydrogen "traffic" to and from the silica support and this offers one possible explanation (63). It may not be as pronounced as over alumina but is certainly impossible on unsupported blacks.

The optimum condition for the overall reaction is a "weighted average" of the individual product classes. Their selectivity values are controlled by both the hydrogen pressure and the catalyst structure. Electron microscopy showed different morphology for the two Pt black catalysts: Pt–N containing "polyhedral" crystals, with more flat planes (2), while Pt–HCHO, sintered at 473 K in H_2 and appearing as aggregates of rounded crystals (64), contained much high-index "miniplanes" (65). The structure of EUROPT-1 was approximated with cubo-octahedra containing 55 Pt atoms (66); both this and the raftlike structures deduced from EXAFS results (67) contain much smaller contiguous Pt surfaces. These different catalyst structures favor different reactions. Hydrogenolysis increased gradually with "step and kink density" over single crystals (68) and hence was attributed to crystal edges. The importance of the so-called B_5 sites (containing five atoms along a step: (110) or (311) "ledge structures") was pointed out for hydrogenolysis on both single crystals and 10% Pt/Al_2O_3 catalysts (69). This reaction was favored in the sequence Pt–N ≥ Pt–HCHO ≫ EUROPT-1 (Fig. 4). The rather ordered crystallites of EUROPT-1 contained fewer "ledge structures" (present as imperfections) than did the big polyhedral particles of Pt–N. This, in turn, must have exposed more "ledges" than did the rounded particles of Pt–HCHO. Aromatization was attributed to structures of threefold symmetry (37a) corresponding to the (111) planes of EUROPT-1 (41), as confirmed by studies on single crystals of similar symmetry (68). Benzene selectivity (Fig. 4) was highest on Pt–N (its larger "flat" planes being likely structurally favorable) and lowest on disperse EUROPT-1 (40, 41). Isomerization and MCP formation was found to be rather structure-insensitive on single crystals (68). Their proposed flat-lying intermediate (1, 70) would require two adjacent metal atoms and could equally take place on the (100) and (111) structures (41). Indeed, the selectivity values for the C_6-saturated products (Fig. 4) were highest on EUROPT-1. Dehydrogenation to alkenes is a structure-insensitive reaction (34, 37b, 68), requiring single atom sites. Its selectivity depends on the possibility of other reactions and plays an important role on partly deactivated catalysts with many Pt–C ensembles (high temperature, low hydrogen pressure), where other reactions are hindered (37b, 40, 41).

We found only small differences in the optimum hydrogen pressure of individual product classes on the three different catalysts (i.e., the maximum $p(H_2)$ of C_6-saturated product formation was a slightly lower over EUROPT-1 than over blacks, while the optimum pressure of benzene showed the opposite behavior). Assuming an adsorbed $C_6H_{13}Pt$ primary intermediate (Scheme 1) and supposing a quasiequilibrium between a less dehydrogenated intermediate of C_5-cyclic reactions and the more dehydrogenated intermediates producing benzene and carbonaceous deposits, it follows that the abundance of these surface entities is governed by the "effective surface hydrogen pressure" (45). This might be about 10 times higher than in the gas phase (45). The actual values of the corresponding adsorption constants must be different on the supported Pt than on Pt blacks, with the same $p(H_2)$ resulting in a higher effective surface hydrogen pressure on EUROPT-1.

The hydrogen pressure dependence of *n*-hexane transformation shows the same picture but with different apparent parameters on the catalysts studied. The conversion and reaction rate values were lower on Pt–HCHO than on Pt–N. Both the presence and position of surface impurities (Table 1) and structural differences (2, 3, 64) can explain the differences.

ACKNOWLEDGMENTS

The authors are grateful to Professor R. Larsson for valuable discussion and advice. Inspiration given by Professor G. C. Bond is thankfully acknowledged. The help of Professor R. Schlögl in making the XPS measurements possible and Ms. Ute Wild for her contribution to their realization is acknowledged. The research received financial support from the Hungarian Scientific Research Fund (Grant OTKA T 025599).

REFERENCES

1. Paál, *Z., Adv. Catal.* **29**, 273 (1980).
2. Paál, Z., Zhan, Z., Fülöp, E., and Tesche, B., *J. Catal.* **156**, 19 (1995).
3. Paál, Z., Xu, X. L., Paál-Lukács, J., Vogel, W., Muhler, M., and Schlögl, R., *J. Catal.* **152**, 252 (1995).
4. Paál, Z., Matusek, K., and Muhler, M., *Appl. Catal.* **149**, 113 (1995).
5. Paál, Z., *Catal. Today* **12**, 297 (1992).
6. Paál, Z., Matusek, K., and Tétényi, P., *Acta Chim. Acad. Sci. Hung.* **94**, 119 (1977).
7. Parayre, P., Amir-Ebrahimi, V., Gault, F. G., and Frennet, A., *J. Chem. Soc., Faraday Trans.* **76**, 1704 (1980).
8. Frennet, A., Lienard, G., Crucq, A., and Degols, L., *J. Catal.* **53**, 150 (1978).
9. Frennet, A., *in* "Hydrogen Effects in Catalysis" (Z. Paál and P. G. Menon, Eds.), p. 399. Dekker, New York, 1988.
10. Bond, G. C., and Slaa, J., *J. Mol. Catal.* **98**, 81 (1995).
11. Bond, G. C., and Slaa, J. C., *J. Mol. Catal.* **89**, 221 (1994).
12. Bond, G. C., and Slaa, J. C., *Catal. Lett.* **23**, 293 (1994).
13. Wootsch, A., and Paál, Z., *J. Catal.* **185**, 192 (1999).
14. Davis, S. M., Zaera, M., and Somorjai, G., *J. Catal.* **85**, 206 (1984).
15. Temkin, M., *Acta Physicochim. URSS* **3**, 312 (1935).
16. Larsson, R., *Catal. Lett.* **36**, 171 (1996).
17. Bond, G. C., *Catal. Today* **49**, 41 (1999).
18. Bond, G. C., *Catal. Rev.* **42**, 323 (2000).
19. Galwey, A. K., *Adv. Catal.* **16**, 247 (1977).
20. Balandin, A. A., *Dokl. Akad. Nauk. SSSR* **93**, 55 (1953).
21. Corma, A., Lopis, F., Monton, J. B., and Weller, S., *J. Catal.* **142**, 97 (1993).
22. Bond, G. C., *Appl. Catal.* **191**, 23 (2000).
23. Bond, G. C., Hooper, A. D., Slaa, J. C., and Taylor, A. O., *J. Catal.* **163**, 319 (1996).
24. Bond, G. C., and Cunningham, R. H., *J. Catal.* **166**, 172 (1997).
25. Bond, G. C., "Catalysis by Metals," p. 139. Academic Press, London/New York, 1962.
26. Rooney, J. J., *J. Mol. Catal.* **129**, 131 (1998).
27. Larsson, R., *J. Mol. Catal.* **55**, 70 (1989).
28. Larsson, R., *React. Kinet. Catal. Lett.* **68**, 115 (1999).
29. Karpinski, Z., and Larsson, R., *J. Catal.* **168**, 532 (1997).
30. Loew, O., *Berichte* **23**, 289 (1890).
31. Paal, C., *Berichte* **49**, 548 (1916).
32. Paál, Z., Schlögl, R., and Ertl, G., *J. Chem. Soc., Faraday Trans.* **88**, 1179 (1992).
33. Baird, T., Paál, Z., and Thomson, S. J., *J. Chem. Soc., Faraday Trans.* **69**, 311 (1973).
34. Paál, Z., Groeneweg, H., and Zimmer, H., *Catal. Today* **5**, 199 (1989).
35. Boudart, M., *in* "Handbook of Heterogeneous Catalysis" (G. Ertl, H. Knözinger, and J. Weitkamp, Eds.), Vol. 3, p. 958. VCH, Weinheim, 1997.
36. (a) Paál, Z., Wild, U., Wootsch, A., Find, J., and Schlögl, R., *Phys. Chem. Chem. Phys.* **3**, 2148 (2001); (b) Find, J., Paál, Z., Sauer, H., Schlögl, R., Wild, U., and Wootsch, A., *Stud. Surf. Sci. Catal.* **130**, 2291 (2000).
37. (a) Biloen, P., Helle, J. N., Verbeek, H., Dautzenberg, F. M., and Sachtler, W. M. H., *J. Catal.* **63**, 112 (1980); (b) Ponec, V., *Adv. Catal.* **32**, 149 (1983).
38. Maire, G., Plouidy, G., Prudhomme, J. C., and Gault, F. G., *J. Catal.* **4**, 556 (1965).
39. Barron, Y., Maire, G., Muller, M., and Gault, F. G., *J. Catal.* **5**, 428 (1966).
40. Paál, Z., Groeneweg, H., and Paál–Lukács, J., *J. Chem. Soc., Faraday Trans.* **86**, 3159 (1990).
41. Bond, G. C., and Paál, Z., *Appl. Catal.* **86**, 1 (1992).
42. Paál, Z., *J. Catal.* **91**, 181 (1985).
43. Paál, Z., and Somorjai, G., *in* "Handbook of Heterogeneous Catalysis" (G. Ertl, H. Knözinger, and J. Weitkamp, Eds.), Vol. 3, p. 1084. VCH, Weinheim, 1997.
44. Sárkány, A., *J. Chem. Soc., Faraday Trans.* **85**, 1523 (1989).
45. Paál, Z., Székely, G., and Tétényi, P., *J. Catal.* **58**, 108 (1979).
46. Rodriguez, N. M., Anderson, P. E., Wootsch, A., Wild, U., Schlögl, R., and Paál, Z., *J. Catal.* **197**, 365 (2001).
47. Bond, G. C., *Appl. Catal.* **149**, 3 (1997).
48. Bond, G. C., Maire, G., and Garin, F., *Appl. Catal.* **41**, 313 (1988).
49. Larsson, R., *Catal. Lett.* **11**, 137 (1991).
50. Larsson, R., *Catal. Lett.* **13**, 71 (1992).
51. Zimmer, H., Rozanov, V. V., Sklyarov, A. V., and Paál, Z., *Appl. Catal.* **2**, 51 (1982).
52. Tétényi, P., *Acta. Chim. Acad. Sci. Hung.* **40**, 157 (1964).
53. Falco, M. G., Canavese, S. A., Comelli, R. A., and Fígoli, N. S., *Stud. Surf. Sci. Catal.* **130**, 2393 (2000).
54. Paál, Z., *J. Catal.* **156**, 301 (1995).
55. Baker, R. T. K., Laubernds, K., Wootsch, A., and Paál, Z., *J. Catal.* **193**, 165 (2000).
56. Gudkov, B. S., Guczi, L., and Tétényi, P., *J. Catal.* **74**, 207 (1982).
57. Gault, F. G., *Adv. Catal.* **30**, 1 (1981).
58. (a) Anderson, J. R., *Adv. Catal.* **23**, 1 (1973); (b) Sinfelt, J. H., *Adv. Catal.* **23**, 91 (1973).

59. Paál, Z., and Tétényi, P., *J. Catal.* **30**, 350 (1973).
60. Teplyakov, A. V., and Bent, B. E., *J. Phys. Chem. B* **101**, 9052 (1997).
61. Wootsch, A., Descorme, C., Paál, Z., and Duprez, D., *in* " Proceedings, 12th International Congress on Catalysis, Granada, 2000" (A. Corma, F. V. Mello, S. Mendioroz, and J. L. G. Fierro, Eds.). Elsevier, Amsterdam, 2000.
62. Sárkány, A., *Catal. Today* **5**, 173 (1989).
63. Duprez, D., *Stud. Surf. Sci. Catal.* **112**, 13 (1997).
64. Paál, Z., Zimmer, H., Günter, R., Schlögl, R., and Muhler, M., *J. Catal.* **119**, 146 (1989).
65. Ehrlich, G., *Adv. Catal.* **14**, 364 (1963).
66. Gnutzmann, V., and Vogel, W., *J. Phys. Chem.* **94**, 4991 (1990).
67. Jackson, S. D., Keegan, M. B. T., McLellan, G. D., Meheux, P. A., Moyes, R. B., Webb, G., Wells, P. B., Whyman, R., and Willis, J., *Stud. Surf. Sci. Catal.* **63**, 135 (1991).
68. (a) Somorjai, G. A., "Chemistry in Two Dimensions: Surfaces," p. 479. Cornell Univ. Press, London, 1981; (b) Blakely, D. W., and Somorjai, G. A., *J. Catal.* **42**, 181 (1976).
69. (a) Garin, F., Aeiyach, S., Légaré, P., and Maire, G., *J. Catal.* **77**, 323 (1982); (b) Dauscher, A., Garin, F., and Maire, G., *J. Catal.* **105**, 233 (1987).
70. Zimmer, H., Dobrovolszky, M., Tétényi, P., and Paál, Z., *J. Phys. Chem.* **90**, 4758 (1986).